

УДК 548.737

## Ciprofloxacinium Malonate Dihydrate: Preparation, Crystal Structure, Thermal Stability

Alexander D. Vasiliev<sup>a,b</sup> and Nicolay N. Golovnev<sup>a\*</sup>

<sup>a</sup> Siberian Federal University,  
79 Svobodny, Krasnoyarsk, 660041 Russia

<sup>b</sup> Kirensky Institute of Physics SB RAS,  
50/38 Akademgorodok, Krasnoyarsk, 660036 Russia

Received 14.11.2012, received in revised form 23.01.2013, accepted 11.02.2013

*Ciprofloxacinium malonate dihydrate (I),  $C_{17}H_{19}FN_3O_3^+ \cdot C_3H_3O_4^- \cdot H_2O$ , ( $C_{17}H_{18}FN_3O_3$  – ciprofloxacin, CfH;  $C_3H_4O_4$  – malonic acid) has been crystallized from the mutual solution of malonic acid and ciprofloxacin in ambient conditions. It has improved aqueous solubility against the ciprofloxacin. The colourless crystals have been investigated using X-ray single crystal and powder techniques, and characterized by differential scanning calorimetry and thermogravimetry. The obtained compound can be considered as a salt with ciprofloxacinium in the role of a cation and malonate as an anion. The compound is crystallized in the triclinic lattice with  $a = 7.283(2)$ ,  $b = 10.090(3)$ ,  $c = 15.104(5)\text{\AA}$ ,  $\alpha = 102.711(4)$ ,  $\beta = 103.328(4)$ ,  $\gamma = 94.261(4)^\circ$ ,  $Z = 2$ ,  $V = 1044.5(6)\text{\AA}^3$ , S.G.  $P\bar{1}$ . The crystal structure determination reveals the importance of inter- and intramolecular interactions in the crystal formation. Thermal behavior and solubility of I provided complementary evidences of salt formation.*

*Keywords: ciprofloxacinium malonate dihydrate, crystal structure, thermal behavior.*

Ciprofloxacin (CfH), 1-cyclopropyl-6-fluoro-4-oxo-7-piperazin-1-yl-quinoline-3-carboxylic acid, is a fluoroquinolone antibiotic approved for the treatment of several types of infections [1]. In aqueous solutions CfH exists mainly in its zwitterionic form, due to the acid base interaction between the piperazine basic nitrogen and the carboxylic group. As a consequence the aqueous solubility of CfH at pHs close to 7 (isoelectric point of the molecule) is low (0.088 mg/ml) [2]. This property makes it difficult to formulate optimized liquid dosage forms such as parenteral, otologic or ophthalmic solutions. Moreover, ciprofloxacin is characterized by a bitter taste [3], which is an additional complication for the oral administration of it. It has been proposed that CfH bioavailability

can be limited by both solubility and permeability [4]. For active pharmaceutical ingredients (APIs) with solubility-limited bioavailability, a challenging task in the development of the product is to improve their solubility without compromising other performance. Indeed, a widely accepted approach to overcome poor solubility of an API is the preparation of their salt forms [5]. Organic salts are generally the preferred crystal form of active pharmaceutical ingredients because of their higher solubility and/or increased degree of crystallinity. Crystalline APIs are strongly preferred due to their relative ease of isolation, the rejection of impurities inherent to the crystallization process and the physicochemical stability that the crystalline solid state affords. The malonic acid is one of active pharmaceutical ingredients [6], and it can be used for preparation soluble forms fluoroquinolone [7].

The aim of this work is to present a new compound  $CfH_2Mal$  ( $Mal^- = C_3H_3O_4^-$ , anion of malonic acid) with improved degree of crystallinity and aqueous solubility.

### Experimental

CfH was obtained from the hydrochloride salt (ciprofloxacin hydrochloride monohydrate,  $CfH \cdot HCl \cdot H_2O$ , Ranbaxia, India, pharmaceutical grade). Ciprofloxacin hydrochloride monohydrate was dissolved in the solution of concentrated ammonia. Then few drops of 4 M HCl were added (pH 8) and white microcrystals of anhydrous ciprofloxacin have precipitated. For the preparation of ciprofloxacinium malonate dihydrate (**I**), a mixture of anhydrous ciprofloxacin (0.20 g, 0.60 mmol) and malonic acid (0.065 g, 0.63 mmol) in water (5 ml) was dissolved. The solution has been kept in a fume hood and colorless crystals have grown in several days. These crystals were used to determine the crystal structure of the compound by X-ray diffraction and to carry on the analysis through the other techniques.

The TG and DSC (Fig. 1) curves show mass losses at least in four steps for **I**. The first mass loss between 80 and 170°C corresponds to an endothermic peak (DSC) and the extremum (DTG) at 90°C is due to dehydration. Estimated (6.37 %) and calculated (7.64 %) mass losses for two water molecule

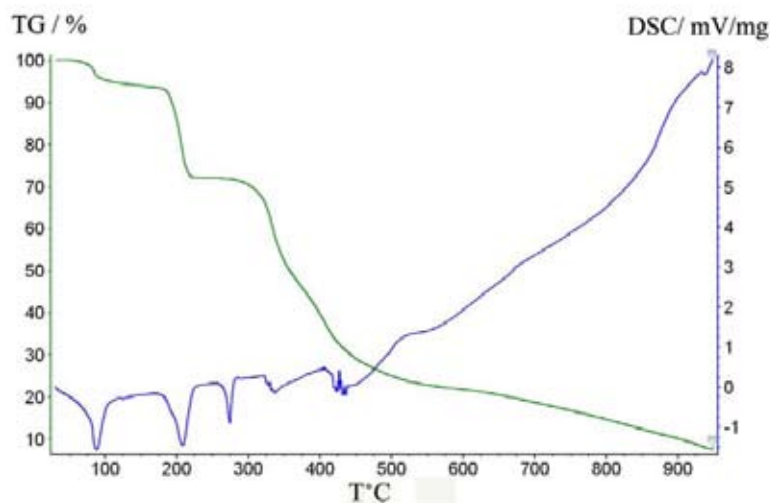


Fig. 1. TG and DSC curves for ciprofloxacinium malonate dihydrate

are in fair agreement. The anhydrous compound is stable up to 190 °C and between 190 and 230 °C the thermal decomposition occurs in a single step. In this step the DSC curve shows a strong endothermic peak at 210 °C. The mass loss (estimated 21.82 % and calculated 22.07 %) corresponds to the lost of malonic acid molecule. The thermal decomposition of this acid occurs with decarboxylation followed by the formation of acetic acid [8]. The constant mass of the substance in temperature range 220-290 °C is received. The third endothermic peak at 278 °C is attributed to the melting of formed ciprofloxacin and its position coincidents with the melting point of ciprofloxacin (277 °C) [9]. Estimated (28.2 %) and calculated (29.7 %) mass losses in this step are in good agreement. The pyrolysis of CfH starts at 290 °C with simultaneous evolution of water and carbon dioxide [9]. The process is not finished at 900 °C (the mass loss is equal to 93 %, Fig. 1).

The solubility of **I** at 298 K was estimated in distilled water using the shake-flask method over 24 h. The concentration of the compound in the filtrate was quantified using UV spectroscopy [10]. The solubility of **I** at 298 K is equal 0.024 M (pH 5.5) that higher than of the corresponding ciprofloxacin [2]. Also, the pH of the malonate solutions is higher than used in pharmacology of the corresponding hydrochloride.

So, the thermal behavior and solubility of **I** provided complementary evidences of salt formation. The product showed improved properties with respect to water solubility and increased degree of crystallinity. This salt would be a good way forward to developing more suitable formulation of this APIs.

Single crystal X-ray diffraction data were collected with MoK $\alpha$  radiation on a Bruker SMART APEX II CCD diffractometer using a crystal sample of dimensions 0.381×0.316×0.260 mm. Experimental absorption corrections were performed using the multi-scan method and the program SADABS [11]. Structure was solved by direct methods using the program complex SHELXS [12] and was refined with the program complex SHELXL [12]. The asymmetric unit of the crystal cell contains ions of CfH $_2^+$ , C $_3$ H $_3$ O $_4^-$  one by one and two molecules of water. All H atoms were subsequently located on difference electron density maps and then refined in idealized positions with constrained mode. The main crystallographic data and refinement parameters are gathered in Table 1.

Due to the presence of NH $_2$  group in CfH $_2^+$ , oxygen atoms in CfH $_2^+$  and in C $_3$ H $_3$ O $_4^-$  as well as H $_2$ O molecules in the structure arose a net of intermolecular H-bonds of N–H $\cdots$ O and O–H $\cdots$ O type which don't involve O3 and O5 atoms only (Fig. 2 and 3). The H-bond paramers are presented in Table 2. The main features of the bonds are centrosymmetric cycles of four water molecules (Fig. 3). Molecules of the cycle are hydrogen bonded with each other and also involved in the same bonds with four C $_3$ H $_3$ O $_4^-$  ions and two CfH $_2^+$  ions. As a result the Ow1 atom is twice hydrogen-bond donor and twice hydrogen-bond acceptor whereas the Ow2 atom is twice hydrogen-bond donor and once hydrogen-bond acceptor.

CfH $_2^+$  ions are packed up in infinite stacks along the crystallographic *a*-axis (Fig. 4) in the crystal. Each stack consists of molecules united in pairs by inversion centers with [n; 1/2; 1/2] coordinates, where n is integer, and the pairs are fastened by two additional C12–H8 $\cdots$ O1 H-bonds (Table 2). The pairs are connected with each other by inversion centers with [n+1/2; 1/2; 1/2] coordinates. As a result, additional supramolecular interactions present at the stack between  $\pi$ -conjugated orbitals of plane molecular cycles; their parameters are shown in Table 3.

Table 1. Experimental details and refinement parameters for  $C_{17}H_{19}N_3O_3F \times 2H_2O$

Chemical formula moiety	$C_{17}H_{19}N_3O_3F \times C_3H_3O_4 \times 2H_2O$
Temperature (K)	298
Space group	$P\bar{1}$
Z	2
$2\theta_{max}$ (°)	52
<i>a</i> , <i>b</i> , <i>c</i> (Å);	7.283(2); 10.090(3); 15.104(5)
$\alpha$ ; $\beta$ ; $\gamma$ (°)	102.711(4); 103.328(4); 94.261(4)
<i>V</i> , Å <sup>3</sup>	1044.5(6)
<i>d</i> , (g/cm <sup>3</sup> )	1.499
$\mu$ , (mm <sup>-1</sup> )	0.124
Reflections measured	8386
Reflections independent	4076
Reflections with $F > 4\sigma_F$	2508
$R_{int}$ / $R_\sigma$	0,030 / 0,049
<i>h</i> , <i>k</i> , <i>l</i> – limits	$-8 \leq h \leq 8$ ; $-12 \leq k \leq 12$ ; $-18 \leq l \leq 18$
Refinement results	
Refinement on $F^2$	$w = 1/[\sigma^2(F_o^2) + (0,0617P)^2 + 0,06P]$ ; $P = (F_o^2 + 2F_c^2)/3$
Refinement parameters	320
$R1$ [ $F_o > 4\sigma(F_o)$ ]	0.0478
$wR2$	0.1371
Extinction coefficient	0.012(2)
Goof	1.04
$(\Delta\rho)_{max}$ , e/Å <sup>3</sup>	0.215
$(\Delta\rho)_{min}$ , e/Å <sup>3</sup>	-0.224
$(\Delta/\sigma)_{max}$	0.000

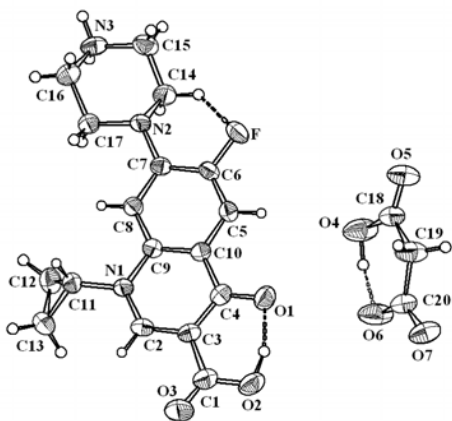


Fig. 2. The structure of  $C_{17}H_{19}N_3O_3F^+$  and  $C_3H_3O_4^-$  with atom numbering scheme. The intramolecular H-bonds are shown as dotted lines

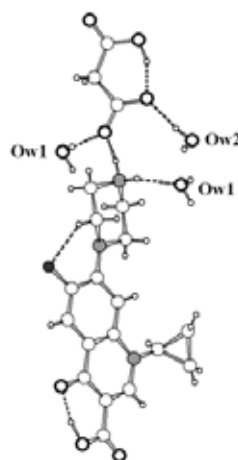


Fig. 3. H-bonds (dotted lines) with the participation of  $C_{17}H_2^+$  and  $Mal^-$

Table 2. Geometrical parameters of H-bonds, D–H...A, and short contacts in the structure. Bond lengths (Å) and angles (°)

D–H	d(D–H)	d(H...A)	∠DHA	d(D...A)	A	transformation for A-atom (acceptor)
O2–H1	0.91(1)	1.65(1)	161(3)	2.531(2)	O1	x, y, z
N3–H2	0.90	1.89	158	2.746(3)	O7	1+x, 1+y, 1+z
N3–H3	0.90	2.00	166	2.880(3)	Ow1	x, 1+y, 1+z
O4–H20	0.91(1)	1.62(2)	159(3)	2.489(3)	O6	x, y, z
Ow1–Hw11	0.90(1)	1.88(1)	168(2)	2.757(3)	Ow2	1–x, –y, –z
Ow1–Hw12	0.90(1)	1.99(1)	161(3)	2.853(3)	O7	x, y, z
Ow2–Hw21	0.90(1)	1.86(1)	171(3)	2.745(3)	O6	1+x, y, z
Ow2–Hw22	0.90(1)	2.04(1)	154(2)	2.875(3)	Ow1	x, y, z
C14–H13	0.97	2.13	129	2.846(3)	F	x, y, z
C12–H8	0.97	2.24	170	3.202(3)	O1	–x, 1–y, 1–z

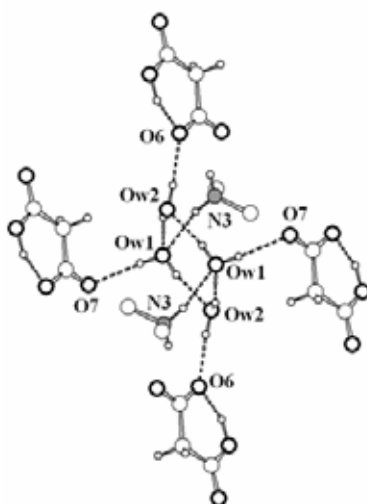


Fig. 4. H-bonds (dotted lines) of water molecules. There shown N3 atom with its environment only instead of  $\text{CfH}_2^+$  ion, for clarity

Table 3. Parameters\* of  $\pi$ – $\pi$ -interactions between  $(\text{cfH}_2)^+$  ions in the structure

$\text{Cg}_i$ – $\text{Cg}_j$	Symmetrical transformation of ring j	d (Å)	$\alpha$ (°).	$\beta$ (°).	$\text{Cg}_i$ _p (Å)	$\text{Cg}_j$ _p (Å)	Slip (Å)
$\text{Cg}_1$ – $\text{Cg}_1$	–x, 1–y, 1–z	3.821(2)	–	23.4	3.5056(9)	3.5057(9)	1.52
$\text{Cg}_1$ – $\text{Cg}_2$	–x, 1–y, 1–z	3.796(2)	2.7(1)	20.2	3.5154(9)	3.5572(9)	–
$\text{Cg}_1$ – $\text{Cg}_2$	1–x, 1–y, 1–z	3.618(2)	2.7(1)	19.9	3.3435(9)	3.4030(9)	–
$\text{Cg}_2$ – $\text{Cg}_1$	–x, 1–y, 1–z	3.796(2)	2.7(1)	22.2	3.5572(9)	3.5154(9)	–
$\text{Cg}_2$ – $\text{Cg}_1$	1–x, 1–y, 1–z	3.618(2)	2.7(1)	22.5	3.4030(9)	3.3435(9)	–
$\text{Cg}_2$ – $\text{Cg}_2$	1–x, 1–y, 1–z	3.680(2)	–	22.5	3.3996(9)	3.3996(9)	1.41

\* d – distance between ring centroids;  $\alpha$  – dihedral angle between planes i and j;  $\beta$  – angle between  $\text{Cg}_i$ – $\text{Cg}_j$  vector and normal to plane i;  $\text{Cg}_i$ \_p – perpendicular distance of  $\text{Cg}_i$  on ring j;  $\text{Cg}_j$ \_p – perpendicular distance of  $\text{Cg}_j$  on ring i; Slip – distance between  $\text{Cg}_i$  and perpendicular projection of  $\text{Cg}_j$  on ring i.  $\text{Cg}_1$ : N1–C2–C3–C4–C10–C9;  $\text{Cg}_2$ : C5–C6–C7–C8–C9–C10.

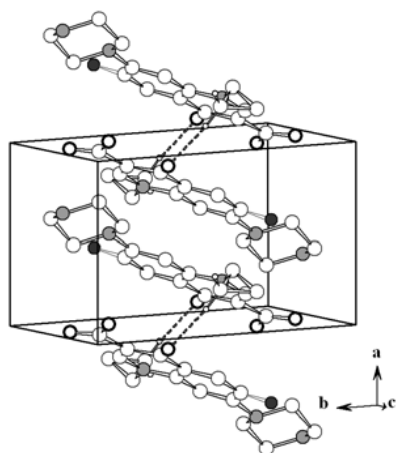


Fig. 5. The molecular packing of the  $\text{CfH}_2^+$  ions in the unit cell. Dashed lines are  $\text{C12-H8}\cdots\text{O1}$  bonds

Table 2. Selected bond distances (Å) and angles (°)

bond	d	bond	d
O1–C4	1.263(3)	O6–C20	1.252(3)
O2–C1	1.324(3)	O7–C20	1.243(3)
O3–C1	1.203(3)	C19–C18	1.493(3)
O4–C18	1.304(3)	C19–C20	1.496(3)
O5–C18	1.205(3)		
angle	$\omega$	angle	$\omega$
O1–C4–C3	122.5(2)	O4–C18–O5	120.8(2)
O2–C1–C3	115.8(2)	O4–C18–C19	121.9(3)
O3–C1–C3	123.6(2)	C18–C19–C20	119.7(2)
O2–C1–O3	120.6(2)	O6–C20–C19	117.5(2)
		O6–C20–O7	124.7(2)

## References

1. Clinical Pharmacology, 2007. Ciprofloxacin [Internet, Restricted Access]. Clinical Pharmacology A Gold Standard Product An Elsevier Company (cited 2009 July 10). Available from: <http://clinicalpharmacology.com/Forms/drugoptions.aspx?cpnum = 127&n = Ciprofloxacin>.
2. Romanuk C.B., Linck Y.G., Chattah A.K. et al. Characterization of the solubility and solid-state properties of saccharin salts of fluoroquinolones // *J. Pharm. Sci.* 2009. V. 98. N 10. P. 3788–3801.
3. Pisal S., Zainnuddin R., Nalawade P. Et al. Molecular properties of ciprofloxacin-indion 234 complexes // *AAPS Pharm. Sci. Technol.* 2004. V.22. N 5, P.1–11.
4. Breda S.A., Jimenez Kairuz A.F., Manzo R.H., Olivera M.E. Solubility behavior and biopharmaceutical classification of novel high-solubility ciprofloxacin and norfloxacin pharmaceutical derivatives // *Int. J. Pharm.* 2009. V. 371. P. 106–112.
5. Romanuk C.B., Linck Y. G., Chattah A.K. et al. Crystallographic, thermal and spectroscopic characterization of a ciprofloxacin saccharinate polymorph // *Int. J. Pharm.* 2010. V.391. P. 197–202.

6. Gauniya A., Das S., Mallick S., Basu S. P. Comparative bioavailability studies of citric acid and malonic acid based aspirin effervescent tablets // J. Pharm. Bioapplied Sci. 2010. V. 2. N 2. P. 18–120.
7. Kruthiventi A.K., Roy S., Gould R. et al. Synergistic Pharmaceutical Cocrystals. WIPO Patent Application WO/2009/136408 Application Number: IN2009/000233 Publication Date: November 12, 2009 Filing Date: April 09, 2009.
8. Caires F.J., Lima L.S., Carvalho C.T. et al. Thermal behaviour of malonic acid, sodium malonate and its compounds with some bivalent transition metal ions // Thermochim. Acta. 2010. V. 497. P. 35–40.
9. Turel I., Bukovec P. Comparison of the thermal stability of ciprofloxacin and its compounds // Thermochim. Acta. 1996. V. 287. P. 311–318.
10. Golovnev N.N., Kirik S.D., Golovneva I.I., Nishnevich M.E. Synthesis and characterization of ciprofloxacin compounds with chlorides of cadmium(II) and mercury(III) // Russ. J. Inorg. Chem. 2006. T.51. N 3. P. 463–468
11. Sheldrick G.M. SADABS. Version 2.01. Bruker AXS Inc. Madison, Wisconsin, USA, 2004.
12. Sheldrick G.M. A short history of SHELX. Acta Cryst. 2008. A64. P. 112–122.

## **Дигидрат малоната ципрофлоксацинума: приготовление, кристаллическая структура, термическая устойчивость**

**А.Д. Васильев<sup>а,б</sup>, Н.Н. Головнев<sup>а</sup>**

*<sup>а</sup>Сибирский федеральный университет,  
Россия 660041 Красноярск, пр. Свободный, 79*

*<sup>б</sup>Институт физики им. Л.В. Киренского СО РАН  
Россия 660036, Красноярск, Академгородок, 50/38*

---

*Дигидрат малоната ципрофлоксацинума (I),  $C_{17}H_{19}FN_3O_3^+ \cdot C_3H_3O_4^- \cdot H_2O$ , ( $C_{17}H_{18}FN_3O_3$  – ciprofloxacin, CfH;  $C_3H_4O_4$  – malonic acid) выделен при взаимодействии в водном растворе малоновой кислоты и ципрофлоксацина при обычных условиях. Полученные бесцветные кристаллы исследованы и охарактеризованы методами монокристалльного РСА, РФА, дифференциальной сканирующей калориметрии и термографии. Соединение I является солью, состоящей из катиона ципрофлоксацинума и малонат-аниона. Оно кристаллизуется в форме триклинных кристаллов с параметрами  $a=7.283(2)$ ,  $b=10.090(3)$ ,  $c=15.104(5)\text{Å}$ ,  $\alpha=102.711(4)$ ,  $\beta=103.328(4)$ ,  $\gamma=94.261(4)^\circ$ ,  $Z=2$ ,  $V=1044.5(6)\text{Å}^3$ , пр. гр.  $P\bar{1}$ . Анализ кристаллической структуры указывает на важность внутри- и межмолекулярных взаимодействий при образовании кристалла. Данные по термической устойчивости и растворимости I подтверждают образование соли.*

*Ключевые слова: дигидрат малоната ципрофлоксацинума, кристаллическая структура, термическая устойчивость.*

---